Anal. Bioanal. Electrochem., Vol. 16, No. 7, 2024, 628-642
https://www.doi.org/10.22034/abec.2024.714686

Analytical & Bioanalytical Electrochemistry

2024 by CEE
www.abechem.com

Full Paper

Polyaniline Ingrained Copper Oxide (PANI/CuO) Nanocomposites for Effective Electromagnetic Interference Shielding and Their Sensitive Detection of Dopamine

Nydile T. Nagaraj,[1] Jadiyappa Sannappa,[1,*] Malathesh Pari,[2] Vasantakumaranaik N. Krishnanaik,[2] Raghavendra Shet,[3] and Madhura Rajashekar[1]

[1]*Department of PG studies and Research in Physics, Kuvempu University Shankaraghatta, 577451, (Karnataka) India*
[2]*Department of PG studies and Research in Industrial Chemistry, Sahyadri Science College Shimoga, 577203, (Karnataka) India*
[3]*Canara First Grade College Mangalore, 575003, (Karnataka), India*

*Corresponding Author, Tel.: +91-9449089870
E-Mail: sannappaj2012@gmail.com

Received: 26 January 2024 / Received in revised form: 28 June 2024 / Accepted: 2 July 2024 / Published online: 31 July 2024

Abstract- In this paper, the electrical conductivity characteristic of polyaniline (PANI) coated CuO nanocomposites of different wt% of CuO nanoparticles can be studied. The synthesis of PANI/CuO nanocomposites was done by in-situ chemical polymerization reaction. Spectroscopic characterizations were done using FTIR, SEM, TGA, XRD, and UV-Vis techniques. The presence of functional groups, surface morphology, and semi-crystalline nature of the sample can be confirmed by FTIR, SEM, and XRD studies. High thermal stability of the sample was confirmed by TGA studies. The frequency-dependent AC conductivity and dielectric attributes of nanocomposites studied at normal room temperature showed tunability with varying wt% of CuO indicating PANI/CuO (5%) exhibits high AC conductivity and dielectric constant values than (10% &15%). It can be observed that the presence of CuO in PANI affects EMI shielding. The synthesized nanocomposites showed excellent EMI Shielding effectiveness of -18.2 dB to -23.1 dB. The results indicate PANI/CuO nanocomposites utilized as potential shielding materials in X-Band. Also, the PANI/CuO/GC electrode expresses good sensing performance for Dopamine. Further PANI/CuO/GCE shows excellent long linear range, sensitivity, and LOD are 10 to 180 µmol/L, 0.0153 and 3.666 and R^2 is 0.9951. Also, this sensor shows repeatability and stability without leaching property.

Keywords- Polyaniline; CuO; AC conductivity; Dielectric permittivity; EMI Shielding; Cyclic Voltammetry; Dopamine

1. INTRODUCTION

With fast increase of electromagnetic pollution because of rising reproduction of instrumentation and electronics, the investigation of substances that can avoid electromagnetic interference (EMI) has noble importance. Electromagnetic interference happens when electronic devices receive electromagnetic radiation emitted by electrical gadgets such as radios, wireless computers, mobile phones, microwaves, etc. [1]. These electromagnetic radiation byproducts can reduce the efficiency, lifetime, and also affect the safety operation of devices. More precisely, an EMI shield in electronic devices controls extreme self-emission of electromagnetic waves and also ensures the undisturbed functioning of devices in the presence of an external electromagnetic field. The metal oxides ingrained conductive polymer nanocomposites piqued researcher's focus in recent years since these composites were awaited to enhance chemical, electrical, structural and electromagnetic properties over their single component its extended uses in several domains [2]. Many metal oxides were noticed from the literature like SnO_2, ZnO, NiO, Fe_2O_3, V_2O_5, MnO and TiO_2 acts as potent dispersants in PANI systems with synergy. CuO has more importance because of its tropical characteristics and increasing applications from gas sensors, heterogeneous catalysts, lightweight battery electrodes, EMI shielding devices, and solar cells. Also, CuO is a n-type semiconductor material with the band gap of 1.5–1.8 eV with a monoclinic structure, and it is having a huge excitation binding energy (60 meV) at normal temperature. Hence, the impact of CuO loading on polyaniline polymer matrix was investigated by the comprehensive study of frequency-dependence electrical conductivity and dielectric attributes [4]. Additionally, integration of CuO nanoparticles into the conductive PANI matrix is expected to form a heterogeneous hybrid system expressing the novel electromagnetic functionalities. The studies illustrate the usage of novel PANI/CuO composites that provide EMI shielding over X-Band [3]. The aim of production of PANI/CuO nanocomposites is applying it as a good charge storage device and in supercapacitor applications and also as a potent EMI Shielding materials in X-Band.

Dopamine is a monoamine compound and it is not only a precursor of norepinephrine (noradrenaline) and epinephrine (adrenaline), is itself a neurotransmitter. In the central nervous system of mammals, dopamine is an essential neurotransmitter, and dopamine loss in the neurons may results in critical diseases such as Parkinson's disorders and schizophrenia. Outside the central nervous system, primarily the DA plays like a local chemical messenger and in blood vessels, it will decrease the rate of norepinephrine discharge and behaves as vasodilator (at standard concentrations). This method suffers from sensitivity, slow electron transfer kinetics and interference from coexisting entities in the body fluid. So as to enhance rate and to decrease fouling effect, electrodes were modified with appropriate entities having capacity to prevail over the preexisting issues [27]. In this research paper prepared novel PANI-CuO/GCE composite material and characterised by various physico-chemical techniques, using this composite material modified GCE to detect the dopamine and it is gives good

analytical profile are linear range, sensitivity and LOD and LOQ as compare to literature reported [28,29].

2. EXPERIMENTAL METHOD

2.1. Materials

Aniline (99% purity), copper turnings, ammonium per sulphate (APS), Conc. HCl, Conc. HNO_3, sodium chloride (NaCl), DMF and double distilled water purchased from Sigma Aldrich.

2.2. Methods

EMI shielding effectiveness of sample can be obtained using Vector Network Analyser at CIF & CMFF IIT Palakkad. AC conductivity was measured by using Impedence analyser. IR Spectra were reported using Shimadzu Spectrometer, UV-Visible Spectrometer were carried out using Shimadzu 1800, TGA of sample was found by SDT Q600 in a N_2 atmosphere at USIC, Karnartaka University Dharwad (KUD). SEM analysis of sample was obtained by JSM-IT500 at SAIF in KUD. XRD analysis was found by single crystal XRD at Tumkur University. The CV were carried out using CHI1608D electrochemical workstation (USA) at SSC shimoga.

2.3. Preparation of CuO nanoparticles and polyaniline (PANI)

5 g of Cu turnings taken in 100 ml jar, 26 ml HNO_3 added slowly. Cu turning undergo oxidation reaction. The dense solution appears bluish green, when adulterated with 500 ml deionised water, the colour of solution turned out to blue. The 10% NaCl added in drops to reaction mixture and stirred. Resultant CuO precipitate filtered and cleansed with deionised water and dried and finally calcinated to obtain CuO nanoparticle. 0.5 M aniline and 0.5 M APS solutions prepared in 0.5 M HCl in two distinct beakers. The prepared solutions stirred under steady magnetic stirring, colourless solution steadily changed to green colour. Solution kept undisturbed and further it was filtered. The darkish green coloured residue finally cleansed with acetone, dried, finely grinded and the powder is called as the conductive PANI [3,5].

2.4. Preparation of polyaniline-copper oxide Nanocomposite

Aniline is dissolved in 1 M HCl. To this reaction mixture different wt% (5%, 10% & 15%) of copper oxide nanoparticles were added and stirred for one hour. To this mixture, APS solution added dropwise with a vigorous stirring period of 4-6 hours at a temperature of 5°C. The washing of the nanocomposites repeated same as in case of PANI alone. The dried powder of reaction product then preserved and utilized for the further characterization [5].

3. RESULTS AND DISCUSSION

3.1. Infrared spectroscopy

The Fourier Transform Infrared Spectroscopy is a very elementary and sensitive analytical mechanism for to identify the composition of organic compounds. FTIR spectrum of CuO, PANI and PANI/CuO nanocomposite were noted using KBr. Figure 1 represents the FTIR spectra of CuO, PANI and nanocomposites of distinct concentration respectively. FTIR of CuO, the peaks which is seen at the wavenumbers 1282 cm^{-1}, 1230 cm^{-1}, 840.52 cm^{-1}, 540.35 cm^{-1} falls under the fingerprint region. The vibration peak at 540.35 cm^{-1} attributed to the strong C-C rocking vibration, 840.52 cm^{-1} indicates to the medium C-C rocking vibration and the peaks at 1282 and 1230 cm^{-1} due to the weak C-O bending vibrations. The FTIR of PANI, the band observed at 1570 cm^{-1} and 1510 cm^{-1} corresponds to the C=N and C=C stretching mode of vibration for quinonoid and benzenoid unit of PANI. The peaks around 1280cm^{-1} are due to the C-N stretching mode of benzenoid ring [6].

Figure 1(a,b,c) represents the FTIR of PANI/CuO nanocomposite of distinct concentrations of CuO nanoparticles. The band which is observed in the range 430-600 cm^{-1} due to Cu-O bending vibration. At 810 cm^{-1} C-H out of plane bending vibration, at 1198 cm^{-1} C-O stretching mode of vibration, at 1499 cm^{-1} C-N stretching of benzenoid ring, the band at 1589 cm^{-1} C≡O vibration, peak between 1810-1905 cm^{-1} carbonyls, at 2103 cm^{-1} C≡C and 2310 cm^{-1} C≡N nitrile, also the peaks seen in between 3500-4000 cm^{-1} is N-H stretching vibration. All the bands are slightly shifted towards the red region. These results attribute the evolution of nanocomposites [7].

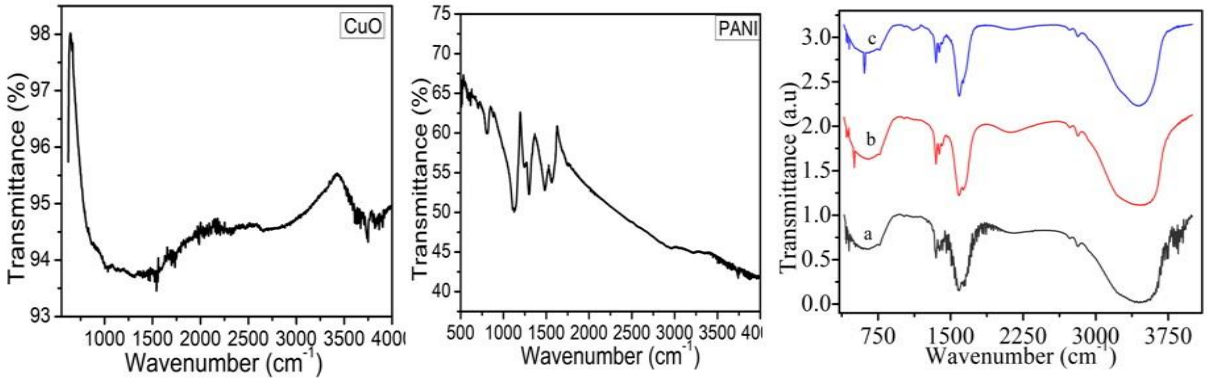

Figure 1. FTIR spectrum of CuO nanoparticles, PANI and different wt.% of PANI/CuO nanocomposites (a) PANI/CuO (15%), (b) PANI/CuO (10%), (c) PANI/CuO (5%)

3.2. Electronic Spectra

The electronic spectrum of PANI/CuO nanocomposite, CuO and PANI were carried out using DMF as the dispersant. In Figure S1, the absorption bands of PANI seen at two distinctive peaks at the wavelength 360 nm and 620 nm, which indicates π-$π^*$ and polaron- $π^*$ transitions

respectively. The characteristic absorption peaks of CuO nanoparticle at 320 nm, 366 nm and 605 nm with a shoulder peak at 423 nm. Which is in agreement with absorption peaks of CuO. The UV-Vis spectra of PANI/CuO nanocomposite of different concentration exhibits the absorption peaks of CuO and PANI. However, the absorption peaks of PANI at 360 nm has shifted to 368nm and the peaks of CuO nanoparticles at 366 nm shifted to 368 nm. Which attributes the insertion of CuO nanoparticles, it has impact on doping of conductive PANI. While this impact owing to interactions at the interface of PANI and CuO. In PANI/CuO nanocomposites, absorption peaks were shifted to higher wavelength that accounts to the decrease of PANI after addition of CuO [8].

3.3. XRD analysis

The structural investigation of PANI/CuO, CuO, PANI can be carried out by using X-ray Diffraction technique. Figure 2a represents XRD of PANI/CuO, CuO and PANI respectively. The XRD Diffractogram of PANI doesn't exhibit any sharp peaks, observed a broad at the diffraction angle 2Ɵ=25º, thus implying the amorphous character of the PANI [28]. In the XRD diffractogram of CuO, the sharp peaks were seen at 2Ɵ=36º, 39º, 48º, 54º also sharp peaks were seen in the range 2Ɵ=54º -80º, thus suggesting the high crystallinity of CuO nanoparticle. The XRD profile of PANI/CuO nanocomposites of distinct concentration exhibiting semi-crystallinity nature carrying a broad peak at 2Ɵ=25º also some of less intense sharp peaks at 2Ɵ=36º, 39º, 48º. This indicating the existence of CuO in the polyaniline matrix. This confirms the formation of polymer nanocomposite [9,11].

Based on the X-Ray peaks broadening the size of crystal can be evaluated using Debye-Scherrer expression and is given by,

$$t = \frac{0.9\lambda}{\beta cos\theta} \qquad (1)$$

where, t =crystalline size of particle, ʎ =wavelength of X-ray, β =FWHM of the peak and Ɵ=Bragg angle.

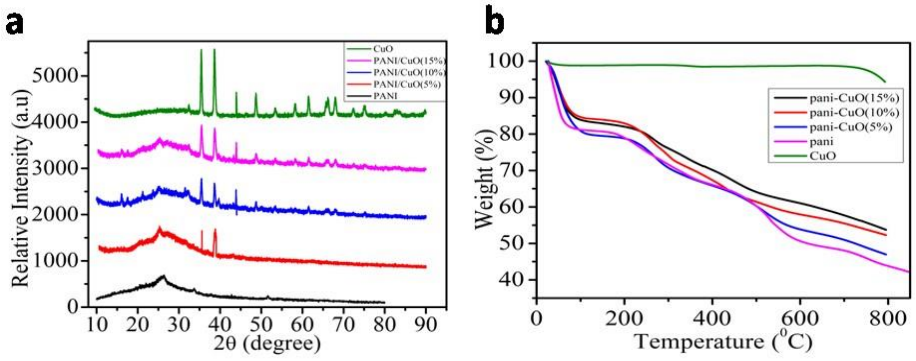

Figure 2. (a)XRD and (b) Thermogravimetric curves of pure PANI, CuO and different wt.% PANI/CuO nanocomposite

3.4. SEM analysis

The surface morphology of synthesized sample can be studied by using Scanning Electron Microscope technique. Figure S2a indicates the SEM image of PANI which shows that PANI has a granular and high porous structure including a high surface area. Figure S2e shows SEM image of CuO, it reveals nanoparticles are fine with the average size of particle is 129 nm. Figure S2(b,c,d) represents SEM imaging of PANI/CuO composites of different loading concentration of CuO on PANI matrix, this indicates doping of CuO NPs has strong impact on PANI polymer morphology. It shows that CuO NPs were well dispersed on PANI matrix with agglomerated morphology. Also, there are some soft blocklike structure which is due to the existence of oxide particles which will increases the crystallinity of composite material [10].

3.5. Thermo gravimetric analysis

Thermogravimetric curves for CuO, PANI and different wt% of PANI/CuO nanocomposites seen in Figure 2b. Thermal degradation is a most essential parameter to understand the influence of nanocomposite formation on the thermal stability of PANI. TG thermogram of pure PANI exhibiting three step weight loss. The first step degradation takes place up to 100ºC due to elimination of H_2O molecules and the moisture. The Second step degradation takes place in between 230º and 380ºC which is owe to loss of dopant molecules. And the third step degradation takes place from 400º-600ºC attributed for thermal degradation of polymeric backbone. Further, TG curve of CuO exhibits very increased thermal stability with less thermal degradation. In addition, TG thermogram of the PANI/CuO nanocomposite showing the similar thermal degradation mechanism as polyaniline with increase in thermal stability [12]. One can observe the shift in degradation temperature towards higher temperature and also PANI/CuO (15%) expressing high thermal stability than other composites with a less weight loss at below 100^0 C and also at higher temperature. This confirms effect of CuO nanoparticles on the Polyaniline matrix and dependency of thermal stability on the concentration of CuO nanoparticles [13].

3.6. Electrical Conductivity Studies

A plot of ac conductivity of pure CuO nanoparticles, PANI and various wt% loading of CuO nanoparticles on PANI matrix [PANI/CuO nanocomposites] vs. frequency at room temperature can be shown in Figure 3. The AC conductivity, dielectric permittivity and dielectric loss can be related by following equation:

$$\sigma_{ac} = 2\pi\varepsilon_0\varepsilon_r f \tan\delta \qquad (2)$$

where, ε_0 is the permittivity of air and ε_r is the dielectric permittivity of the sample, f is the frequency and tan δ is the dielectric loss.

It is observed that at lower frequency PANI/CuO nanocomposites indicates frequency dependent AC conductivity even above 100 Hz. It is noticed that for each PANI/CuO sample there is an increase in the electrical conductivity with an applied external frequency of electric field [14]. Which is mainly owing to interfacial polarization [15]. Which suggests that at lower frequency of applied field very less number of charge carriers can be capable to cross the potential barrier leading to lower electrical conductivity of the sample. For the higher frequency, the σ_{ac} increases due to the tunneling of charge carriers, they get enough energy to overcome the potential barriers. As a similar response can be noticed polymer nanocomposites [16].

The σ_{ac} decreases with the increase in loading of CuO wt% in PANI matrix for all the frequencies. It is evident that by SEM images and XRD spectral studies reduction in ac conductivity is owing to the rise in the disorderliness in nanocomposites, this will result into the conformational changes in Polyaniline matrix by shortened delocalization length. The variation of dielectric permittivity of CuO and PANI/CuO nanocomposites with frequencies from 40Hz to 5MHz can be shown in Figure S3. The higher value of dielectric permittivity ε^1 is observed in the lower frequency region owing to the contribution of all kinds of polarization via, ionic, electronic, space charge, and orientational polarization mechanisms.

There is a decrease of dielectric permittivity ε^1 with the increase in alternating frequency which is ascribed to the fact that the variation in the field is very rapid for which the dipoles do not have sufficient time to align themselves to the applied field [17,27]. So that electronic polarization only contributes, remaining all other polarization seizes. Also, the dielectric permittivity falls with the rise in wt% CuO upon loading of CuO nanoparticles on polyaniline matrix, the interchain distance will increase resulting into the decrease in dielectric permittivity and hence the electrical conductivity of nanocomposite [18]. The frequency-dependent dielectric tangent loss of PANI with different wt% loading CuO is indicated in Figure S4. The tangent loss (tanδ) for composites is remarkably modified upon incorporation of CuO [10].

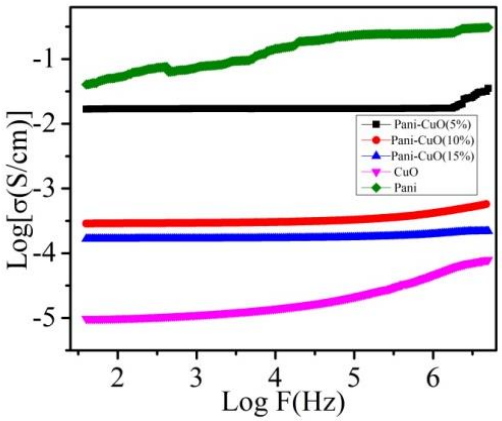

Figure 3. Variation of AC conductivity with frequency of PANI, CuO and PANI/CuO nanocomposites.

3.7. EMI Shielding analysis of PANI/CuO nanocompsites

EMI Shielding effectiveness of any shielding material be capability to generate significant attenuation of EM energy incident on material and distinct relevant parameters like Reflection coefficient (R), Absorption coefficient (A) & Transmission coefficient (T) can be measured with the help of scattering parameters (S-parameters) S_{11} and S_{21} [19]. The operation involved in EMI Shielding shown in Figure S5. EMI SE due to reflection can be represented as:

$$SE_R = -10\log(1-R) \quad (3)$$

The EMI SE due to absorption is:

$$SE_A = -10\ \log\ (\frac{T}{1-R}) \quad (4)$$

where, R=S_{11}^2 and T=S_{21}^2 The total shielding effectiveness (SE_T) is sum of shielding effectiveness due to reflection (SE_R), absorption (SE_A) and multiple reflections (SE_M) is expressed as: $SE_T = SE_A + SE_R + SE_M$[3]. If $SE_T > -10$dB then SE_M can be negligible as multiple reflection component leads to the overall EM energy absorption, SE_T can be given by

$$SE_T = SE_A + SE_R \quad (5)$$

The EMI shielding effectiveness (SE) of PANI/CuO composites of different wt% of CuO in X-Band (8.2-12.4 GHz) can be shown in Figure 4. As noticed from various literatures, several researchers probed and stated the EMI SE of PANI ranges between -13dB to -14 dB. In this work, EMI shielding values of PANI/CuO nanocomposites in X-band (8.2-12.4 GHz) are acquired in range of -18.2 dB to -23.1 dB [20]. According to electromagnetic compatibility regulations (EMC), EMI SE in range -20 dB exhibits 99% of electromagnetic energy will be attenuated by shielding materials [26]. Therefore, attained SE in the X-Band validated that, PANI/CuO nanocomposites is enhanced as efficient shielding substance for the vast range of frequencies. The enhancement of SE very clearly elucidates impact of CuO addition in Polyaniline polymer matrix. The largest SE value -23.1dB exhibited by PANI/CuO (15%). Figure 5a depicts the impact of concentration (wt%) of CuO in PANI for noticed enhancement in SE at distinct opted frequencies in X-Band [3]. From the graphs, it is noticed that, as CuO(wt%) content increases the SE also rises and utmost effectiveness -23.1dB can be attained at 15 wt% of CuO content [20]. Accordingly, all these replies of nanocomposites are in direction of attenuation of EM energy.

Figure 5b indicates microwave reflection coefficient (R) and absorption coefficient (A) in the broadband frequency region 8.2-12.4 GHz. This presents a direct detail about the particular mechanism of attenuation of EM energy. The obtained result reveals that all nanocomposite samples have marginal dominancy in the direction of absorption with a credible reflection ability. The variation of the absorption coefficient of all nanocomposite samples is in the range of 0.525 to 0.6, whereas the reflection coefficient (R) changes in the range of 0.4 to 0.46. The obtained outcomes are pertinent as there is an increased need for shielding materials with a

balanced attenuation ability of EM energy through both reflection and absorption [3]. The potent nanocomposite hybrid network allowed the charge carrier to dissipate and reflect the EM energy by absorption through the mechanism of polarization [21].

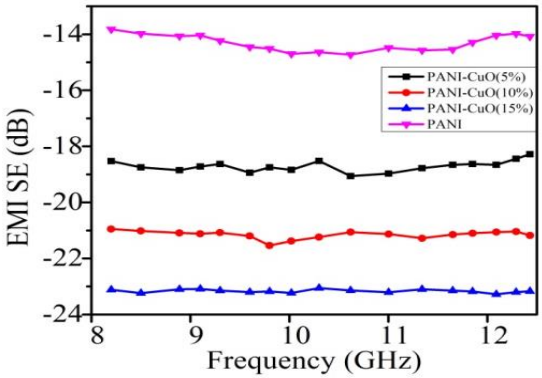

Figure 4. Variation of EMI shielding effectiveness (SE) of PANI/CuO nanocomposites of different wt% and PANI with Frequency in X-band

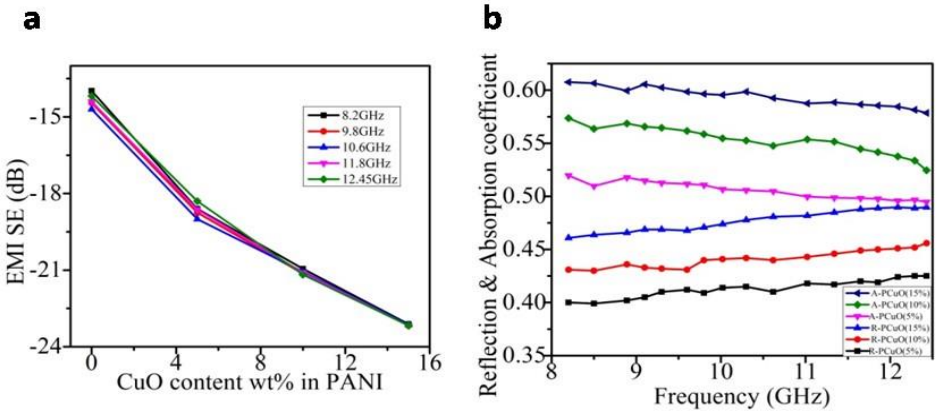

Figure 5. (a) Variation of EMI SE as the function of wt% of CuO in polyaniline (b) Variation of Absorption coefficient (A) and Reflection coefficient (R) as the function of frequency

Table 1. Comparative studies of EMI Shielding properties of various reported materials under optimal conditions

Material	**Frequency**	**SE_T (dB)**	**Thickness**	**Reference**
PANI-CuO	12.4-18GHz	~ -21	2mm	[3]
polyaniline-$NiFe_2O_4$:Cu	0 - 8GHz	~ -29.74	2mm	[22]
Polyaniline-MWCNT	8.2-12.4GHz	~48	2mm	[23]
PANI-Molybdate	8.2-12.4GHz	~ -14	2mm	[24]
PANI-CuO (5%, 10%,15%)	8.2-12.4GHz	~ -18.2 to -23.1	2mm	Present work

The effective polaron and bypolaron movement in PANI/CuO nanocomposite aided to absorption and also a reflection of microwave energy [22-24]. The rise in CuO concentration content in the polyaniline matrix commenced the marginal rise in the reflection mechanism [25]. The comparative studies of EMI Shielding property of various reported materials under optimal conditions are shown in Table 1.

3.8. Electrochemical Characterization

3.8.1. Preparation of modified glassy carbon electrode

0.5 mg of PANI-CuO/GCE taken in IPA (isopropanal) solvent were sonicated of 30 min and the 5 µL of the finely dispersed solution was drop coated on the previously cleaned and dried GCE and the electrode surface dried at normal room temperature under ambient conditions.

3.8.2. Charge transfer performance of modified electrodes

The cyclic voltammetry (CV) studies can be undertaken to confirm the sensing capability of PANI-CuO/GCE. The different modified GCE was carried out in 0.1 M KCl solution having 0.5 mM $K_4[Fe(CN)_6]$ indicated in Figure S6 to get an insight into the electrode electro-active behavior. Bare GCE exhibited the lowest redox current intensity, when PANI-CuO/GCE was immobilized on the electrode surface area the redox current intensity got intensified as contrast to the bare electrode. It indicates effective conductivity because of an electron transfer resistance. The study disclosed PANI-CuO/GCE modified electrode is an effective electrode for electrochemical studies [30].

3.8.3. Electrocatalytic properties of the different electrode

The voltammetric response of DA was noticed using CV. Figure S7a exhibits CV of PANI-CuO/GCE in PBS (pH 7.0). No redox peaks in the potential range 0 to 0.6 V were seen. After the addition of 10 µl DA into PBS, a sensitive quasi-reversible peak was observed at a potential 350 mV (Figure S7b). This effect implies PANI-CuO/GCE has good electro-catalytical activity towards the oxidation of DA. Quasi-reversible peak current seen on reverse scan, expressing processing of DA on PANI-CuO/GCE electrode is a Quasi reversible process. CV utilized to assess the electrocatalytical response of DA towards a distinct class of modified electrodes are PANI-CuO/GCE, and modified electrodes with DA analyte indicated in Figure S7. The oxidation peak current of DA on PANI-CuO/GCE clearly raised and the oxidation peak potential shifted towards negative [31,36]. The anodic peak potential negatively shifted by 460 mV than PANI-CuO/GCE (Figure S7b). This effect reveals PANI-CuO/GCE has a strong electrocatalytic effect towards oxidation of DA [32].

3.8.4. Electrocatalytic behavior of PANI-CuO/GC electrode towards DA

CV of DA at PANI-CuO/GCE electrode in a buffer solution of pH 7.0 has been shown in Figure 6. The voltammograms exhibited a redox peak at the modified electrode with potential values of anodic and cathodic peaks of 345 mV and 204 mV respectively. Because of the electrostatic interaction between DA and positively charged modifier [31,32]. Upon the ideal situation, PANI-CuO/GCE electrode caused a remarkably larger peak current and provides direct proof of catalytic effect [35].

Figure 6a indicates voltammogram of variation of DA concentration at PANI-CuO/GCE electrode in buffer solution of pH 7.0 disclosed that there is a linear growth in both cathodic peak current and anodic peak current with rise in DA proportion and a small switch in peak potential towards negative side. Linearity observed between dopamine concentration variation and anodic peak current with correlation co-efficient value 0.9951. And further the modified electrode shows very good analytical profiles are long linear range, sensitivity and LOD are 10 to 180 µmol/L, 0.0153 and 3.666 and R^2 is 0.9951 [36].

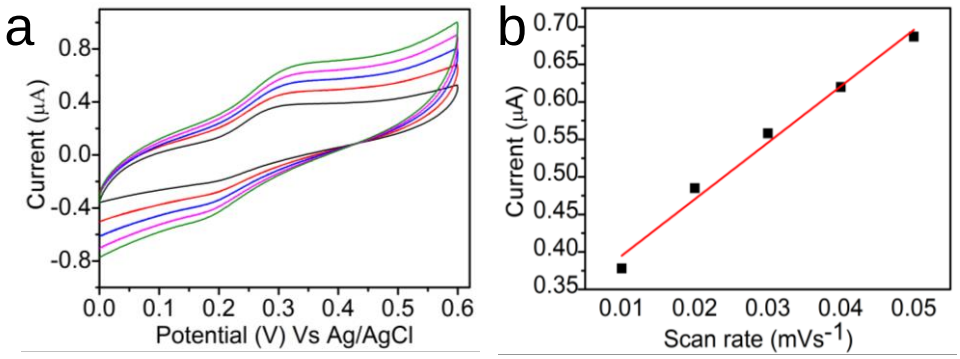

Figure 6. a) CVs of the CuO-PANI/GCE electrode in PBS (pH 7.0) with different concentrations of DA, scan rate: 50 mV/s, b) Inset linear graph of concentration versus current

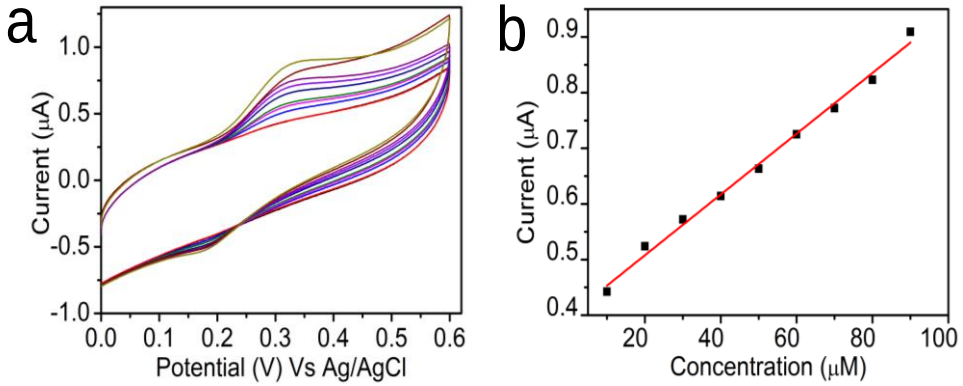

Figure 7. a) Cyclic voltammogram of dopamine at scanning rate ranging from (10 mV^{-1} to 50 mVs^{-1}), b) Inset: Calibration graph of peak current vs scan rate

3.8.5. Impact of scan rate on electrocatalytic capability of DA

CVs for DA in a PBS at PANI-CuO/GCE electrode showed a pair of quasi-reversible peaks is shown in Figure 7a. The oxidation peak current raised with increasing scan rate, in the range from 10 to 50 mVs^{-1} the redox peak current was proportional to the scan rate. The plot of peak current vs scan rate for DA in Figure 7b showed a linear relationship and the straight-line equation is represented by Y=10.58(DA)+1.082 with a correlation coefficient of R^2 =0.9945. The linear graph of peak current versus scan rate inferred that electrode reaction is an adsorption-controlled process [29].

Table 2. Comparison of the results for the DA with the literature reports

Electrode material	**Linear range (µmol/L)**	**Technique**	**LOD (µmol/L)**	**Sensitivity**	**Reference**
poly(l-arginine)/CPE	50-100	CV	0.5	-	[30]
rGO-Zn(II)TPEBiPc	0.02-1.0	CV	0.006	2.8784	[31]
Co(II)HTC/GCE	0.2 - 10	CV	0.066	1.069	[32]
MWCNT-[Co(DPD)2Cl2]/GCE	0.2-10	CV	0.066	1.65	[33]
Azo-bridged Cu(II)Pc	2-140	CA	0.66	-	[34]
PANI-CuO/GCE	10 –130	CV	3.666	0.0153	This work

3.8.6. Reproducibility and repeatability Studies

To examine the repeatability of the modified electrode, PANI-CuO/GCE replies corresponding to 40 µM DA analyte were recorded 60 times. The standard deviation and Efficiency variation were measured to be 0.2% and 0.038. Apart, modified GCE presents 94.6% of first response current even after four weeks of storage, proving the remarkable storage stability of modified electrodes [34]. Results present that our PANI-CuO/GCE-modified electrodes have excellent stability, sensitivity, and repeatability. PANI-CuO/GCE synthesized compounds characterized by electrochemical and spectral methods are given in Table 2. Besides this, electro-analytical and spectral conduct of CuO-PANI/GCE biomolecules.

3.8.7. Analysis of dopamine injection sample

Relevance of the modified GCE as an electrochemical sensor carried out for the effective detection of DA hydrochloride injection. The measure of the concentration of DA hydrochloride in injection can be done by using a calibration plot with the help of methods suggested in the effect of concentration in standard DA. Results acquired after the standard addition procedure are shown in Table 3.

Table 3. Determination of DA in dopamine hydrochloride injection

Sample No.	Spiked DA (mg)	Found (mg)	Recovery	RSD
1	0	0.048±0.001	98.8	2.32
2	4	3.89±0.02	97.25	2.43
3	4	3.6±0.01	90.0	3.32
4	4	3.9±0.04	97.0	2.20
5	4	3.7±0.05	92.0	2.64
6	4	3.8±0.03	95.0	2.47

The recoveries from 97 to 105.5% of DA secured for dopamine hydrochloride injection samples (n= 5 repetitions). It is proof of the accuracy of the suggested procedure. Statistical calculations for obtained results depicted excellent precision for the CV method, showing PANI-CuO/GCE modified electrode used for sensing dopamine hydrochloride injection samples [32,37].

4. CONCLUSION

The synthesis of PANI/CuO is carried out by in-situ chemical polymerization reaction. The spectroscopic characterization of synthesized samples can be done using FTIR, XRD, SEM, TGA, and UV-Vis techniques. The PANI/CuO of different wt% exhibits a semi-crystalline nature and the crystallinity of CuO nanoparticles is not disturbed in the PANI matrix. The synthesized composite exhibits a very good thermal stability, the obtained results suggest that as the CuO wt% increases the thermal stability also increases. The electrical conductivity response with frequency can be studied indicating the electrical conductivity is higher for the PANI/CuO (5%) as compared to PANI/CuO (10,15%). Also, as the CuO% increases in the PANI matrix the inter-chain distance increases so it reduces both electrical conductivity and dielectric permittivity. The results depict that the synthesized PANI/CuO nanocomposite can act as a good semiconducting material that can be used in supercapacitor applications and batteries. The EMI SE of nanocomposites in X-band indicates that synthesized samples exhibit excellent EMI SE ranges from -18.2 dB to 23.1 dB. Also, the incorporation of CuO on PANI matrix affects the EMI SE value. As the concentration of CuO nanoparticles on PANI increases the EMI SE also increases. Hence, the synthesized nanocomposites can be potent EMI shielding materials in various electronic devices and applications. Additionally, the synthesized PANI-CuO/GCE can be used in the determination and sense of Dopamine and also in the real samples i.e., Dopamine hydrochloric injection. All these results indicate PANI-CuO can be an excellent energy storage material with a high sensing performance of dopamine.

Acknowledgments

The authors wish to acknowledge the CIF & CMFF, IIT Palakkad for Electromagnetic interference shielding data, the Karnataka University Dharwad & Sahyadri Science College Shimoga for imparting spectral data.

Declarations of interest

The authors have no conflict of interest.

REFERENCES

[1] S. Geetha, C.R.K. Rao, K.K. Satheeshkumar, and M. Vijayan, J. Appl. Polym. Sci. 112 (2009) 4.

[2] L. Omana, A. Chandran, R.E. John, R. Wilson, and K.C. George, ACS Omega 7 (2022) 25921.

[3] N. Maruthi, M. Revanasiddappa, and B.P. Prasanna, Colloids & Surf A: Physicochem. Eng. Asp. 621 (2021)126611.

[4] R. Basapathi, T. Sankarappa, and A. Malge, J. Inorg & Organometallic Polym. Mater. 32 (2022) 5.

[5] B. Raghavendra, T. Sankarappa, and A. Malge, Conf. Proc. Mater. Sci. Eng.1248 (2022) 012002.

[6] M. Nagaraja, P. Sushma, H.M. Mahesh, and K. Rajanna, Mater. Today: Proc. 49 (2022) 1989.

[7] L.N. Shubha, M. Kalpana, and P.M. Rao, Conf.: Frontier in Chem. Res. & Analysis (2015) 24.

[8] L.I. Nadaf, and K.S. Venkatesh, Mater. Sci. Res. India 12 (2015) 108.

[9] D.S. Bai, and R.P. Suvarna, Indian J. Sci. Technol. 10 (2017).

[10] H.K. Inamdar, D. Mahalesh, R. Siddanna, M.V.N. Ambikaprasad, and R.D. Mathad, Intern. J. Res. Eng. Technol. 5 (2016) 99.

[11] V.S. Desouza, H.O. Frota, and E.A. Sanches, J. Mol. Struct. 1153 (2017) 20.

[12] A.G.N. Sofiah, M. Samykano, K. Sudhakar, and A.K. Pandey, J. Mol. Liq. 375 (2023) 121303.

[13] M.M.R. Khan, Y.K. Wee, and Mahmood, Inter. J. Chem. Reactor. Eng. 12 (2014) 1.

[14] D. Sharma, B.S. Kaith, and J. Rajput, Sci. World J. 2014 (2014) 904513.

[15] B. Kaur, R. Tanwar, and U. Mandal, Colloids and Surf. A: Physicochem. Eng. Asps. 599 (2020) 124798.

[16] M.A. Sangamesha, K. Pushpalatha, and G.L. Shekar, Indian J. Adv. Chem. Sci, 2 (2014) 223.

[17] R. Anitha, E. Kumar, K. Rathnakumar, and S.C. Vella Durai, J. Ovo. Res, 17(2021)99.

[18] Y. Li, M. Zhou, Z. Xia, Q. Gong, X. Liu, Y. Yang, and Q. Gao, Colloids and Surf. A:

Physicochem. Eng. Asps. 602 (2022) 125172.
[19] R.R. Mohan, A. Abhilash, M. Mani, and S.J. Varma, Mater. Chem. Phys. 290 (2022) 126647.
[20] K.G. Gareev, V.S. Bagrets, V.A. Golubkov, and M.G. Ivanitsa, Optical & Quantum Electronics 9 (2020) 734.
[21] S.S. Afzali, S.H. Hekmatara, and J.S. Yazdi, Sci. Rep. 12 (2022) 9590.
[22] E.I. Sahin, M. Emek, J.E.F.M. Ibrahim, and M. Kartal, Optical & Quantum Electronics 55 (2023) 500.
[23] R. Pal, S.L. Goyal, I. Rawal, and V. Gupta, J. Phy. Chem. Solids 169 (2022) 110867.
[24] M.N. Taj, B.D. Prasad, N. Ramarao, and H. Nagabhushana, Appl. Surf. Sci. Adv, 7 (2022) 100203.
[25] D.S. Rahul, T.P.M. Pais, N. Sharath, S.A. Ali, and M. Faisal, AIP Conf. Proc. 1665 (2015) 140021.
[26] L. Lyu, J. Liu, K. Sun, R. Fan, and N. Wang, Eng. Sci. 2 (2018) 26.
[27] V.P. Elanjeitsenni, K.S. Vadivu, and B.M. Prasanth, Mater. Res. Exp. 9 (2022) 022001.
[28] H. Meskher, F. Achi, and H. Belkhalfa, J. Compo. Compos. 4 (2022) 13.
[29] N. Ranjitha, G. Krishnamurthy, H.S. Bhojya naik, M. Pari, L. Afroz, K.R. Sumadevi, and M.N. Manjunatha, Inorg. Chemi. Acta 543 (2022) 121191.
[30] B.N. Chandrashekar, K. Swamy, M. Pandurangachar, T.V. Sathisha, and B. Sherigara, Colloids Surf. B 88 (2011) 413.
[31] M. Pari, K.R. Venugopala Reddy, Fassiulla, and K.B. Chandrakala, Sens. Actuator A 316 (2020) 112377.
[32] L. Afroz, M.H. Moinuddin Khan, H.M. Vagdevi, M. Pari, R. Mohammed Shafeeualla, and K.M. Mussuvir Pasha, Emergent Mater. 5 (2021) 1133.
[33] M. Pari, M. Nayaka, and K.R.V. Reddy, Anal. Bioanal. Electrochem. 11 (2019) 460.
[34] P. S. Kumar, B. S. Sreeja, K. K. Kumar, and G. Padmalaya, Food Chem. Toxicol. 167 (2022) 113311.
[35] M. Maulidiyah, T. Azis, L. Lindayani, D. Wibowo, A. Aladin, and M. Nurdin, J. Electrochem. Sci. Technol. 10 (2019) 394.
[36] F. Li, B. Ni, Y. Zheng, Y. Huang, and G. Li, Surf. Int. 26 (2021) 101375.
[37] T. S. Anirudhan, and J. R. Deepa, J. Colloid Int. Sci. 490 (2017) 343.

Copyright © 2024 by CEE (Center of Excellence in Electrochemistry)

ANALYTICAL & BIOANALYTICAL ELECTROCHEMISTRY (http://www.abechem.com**)**

Reproduction is permitted for noncommercial purposes.